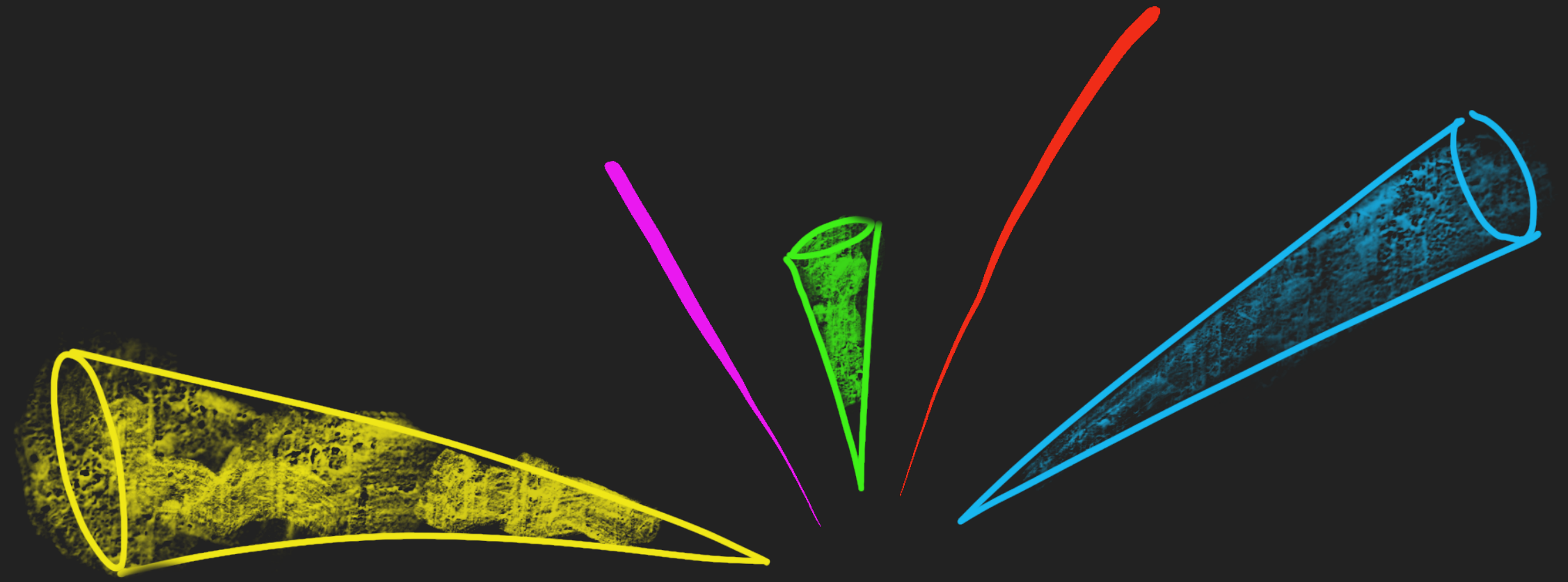


Machine learning techniques for cross-section measurements for the vector-boson-fusion production of the Higgs boson in the $H \rightarrow WW^* \rightarrow e\nu\mu\nu$ decay channel with the ATLAS detector

57th Rencontres de Moriond

23rd March, 2023

Sagar Vidya Addepalli



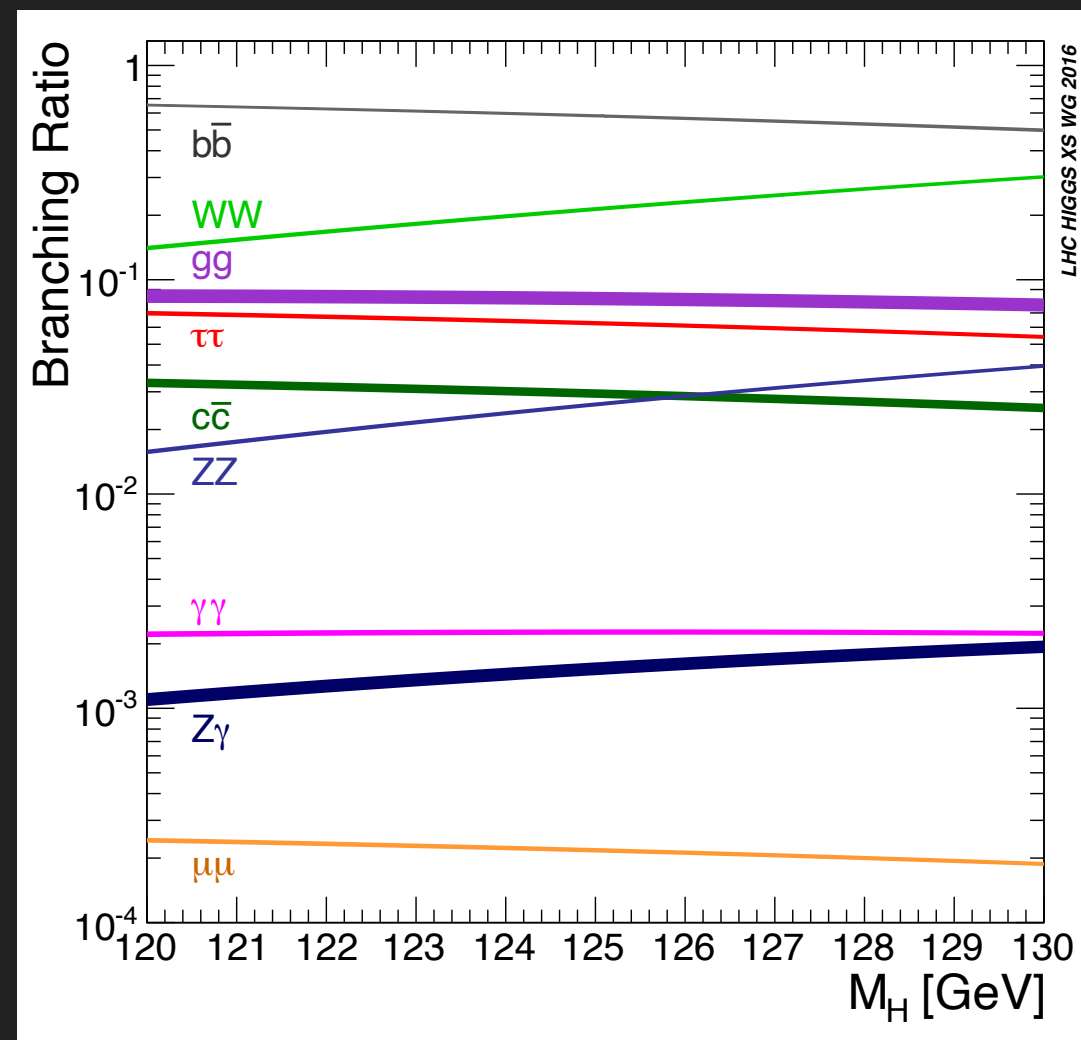
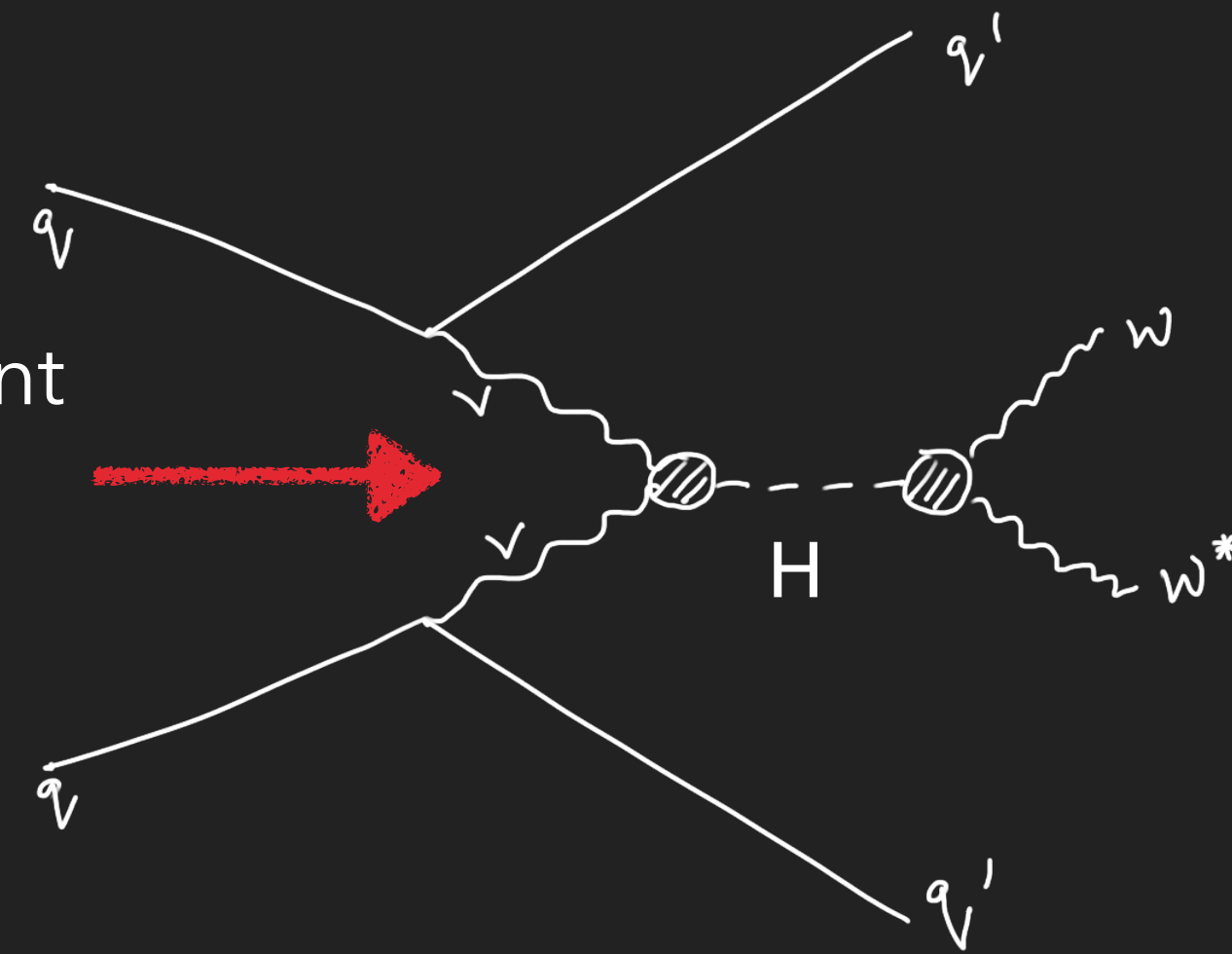
Brandeis



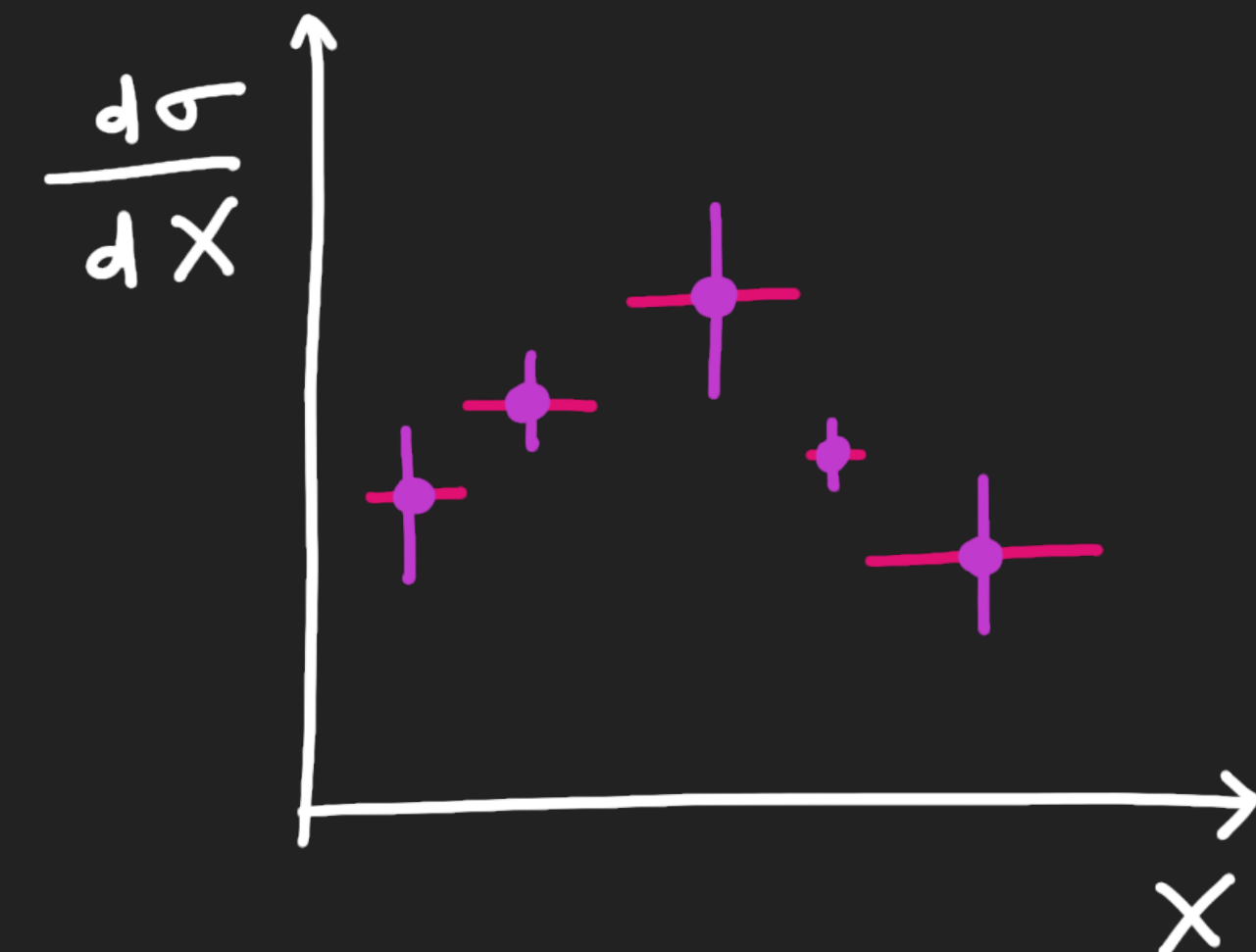
ATLAS
EXPERIMENT

Understanding the **fundamental properties of the Higgs boson** is one of the main goals of the physics programme at the LHC.

VBF cross-section measurement probes directly the **Higgs coupling to W and Z bosons**.



$H \rightarrow WW^*$ has a high BR (~20%) and good signal purity



Differential XS sensitive to many properties of the Higgs – spin & CP structure, anomalous couplings.

Measurement extremely challenging:

- Final state not fully reconstructed – **non-resonant signal**
- **Signal/Background of 0.13** in the targeted phase space

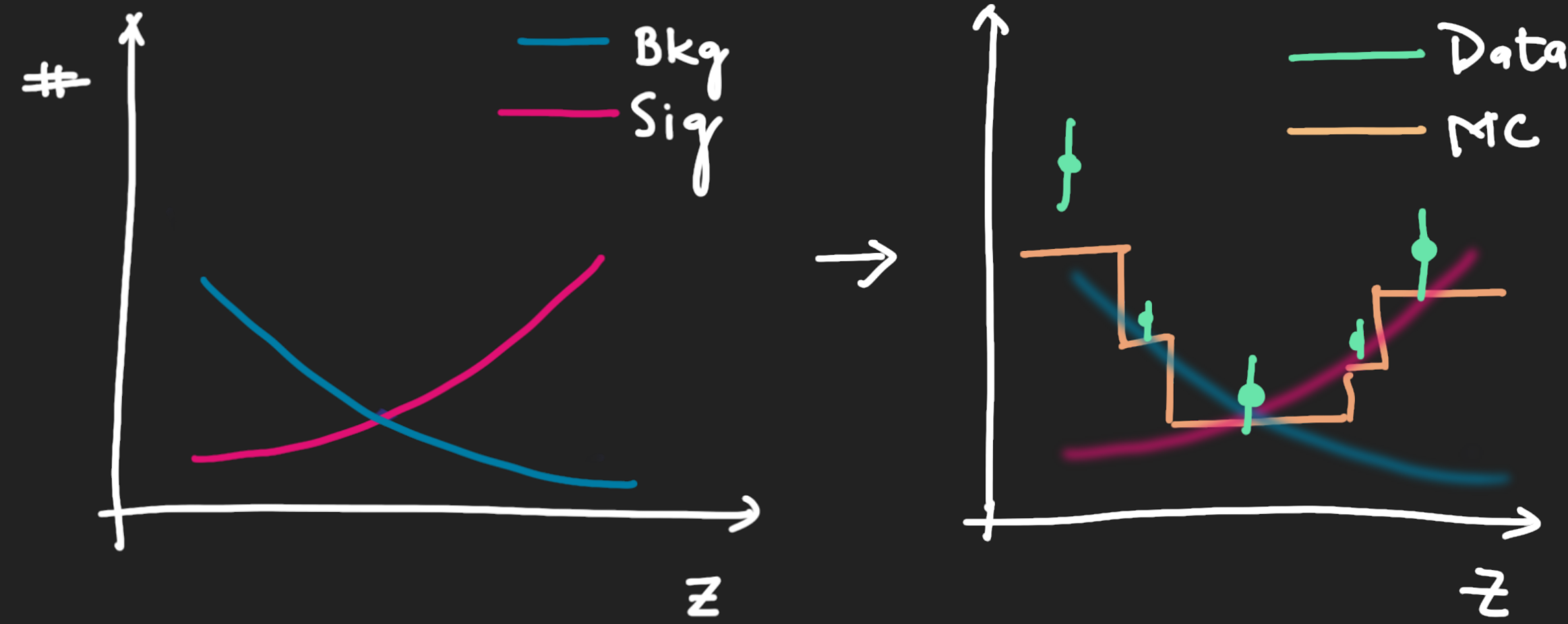
To maximize signal sensitivity:

- **Boosted Decision Trees** output used as classifiers
- Classifiers used as **templates** in the multi-dimensional fit



To minimize model dependency with BDTs:

- BDTs **trained in a broader phase space** than what is measured
- Retrained with a **smaller set of variables** for each differential XS measurement



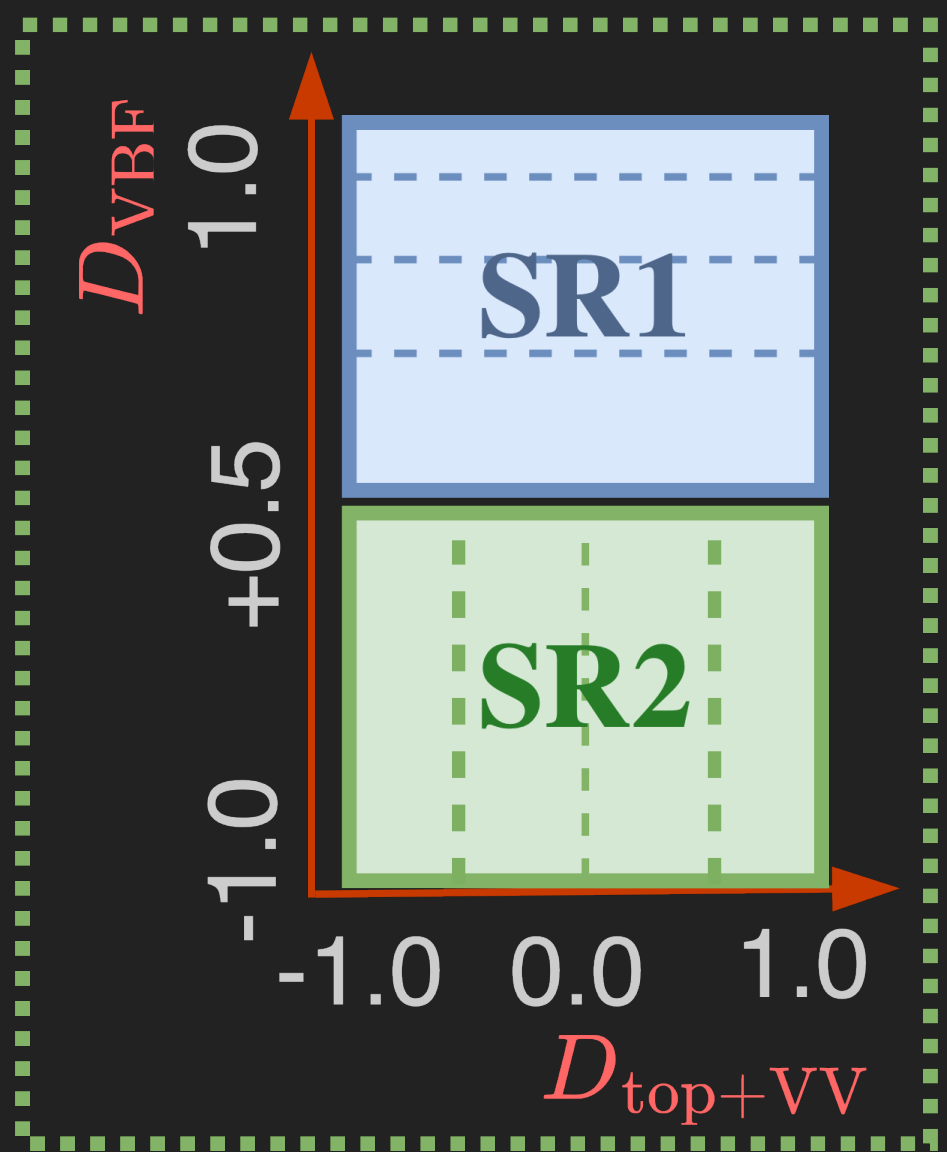
Multi-dimensional fit using a multivariate discriminant

SIGNAL EXTRACTION STRATEGY

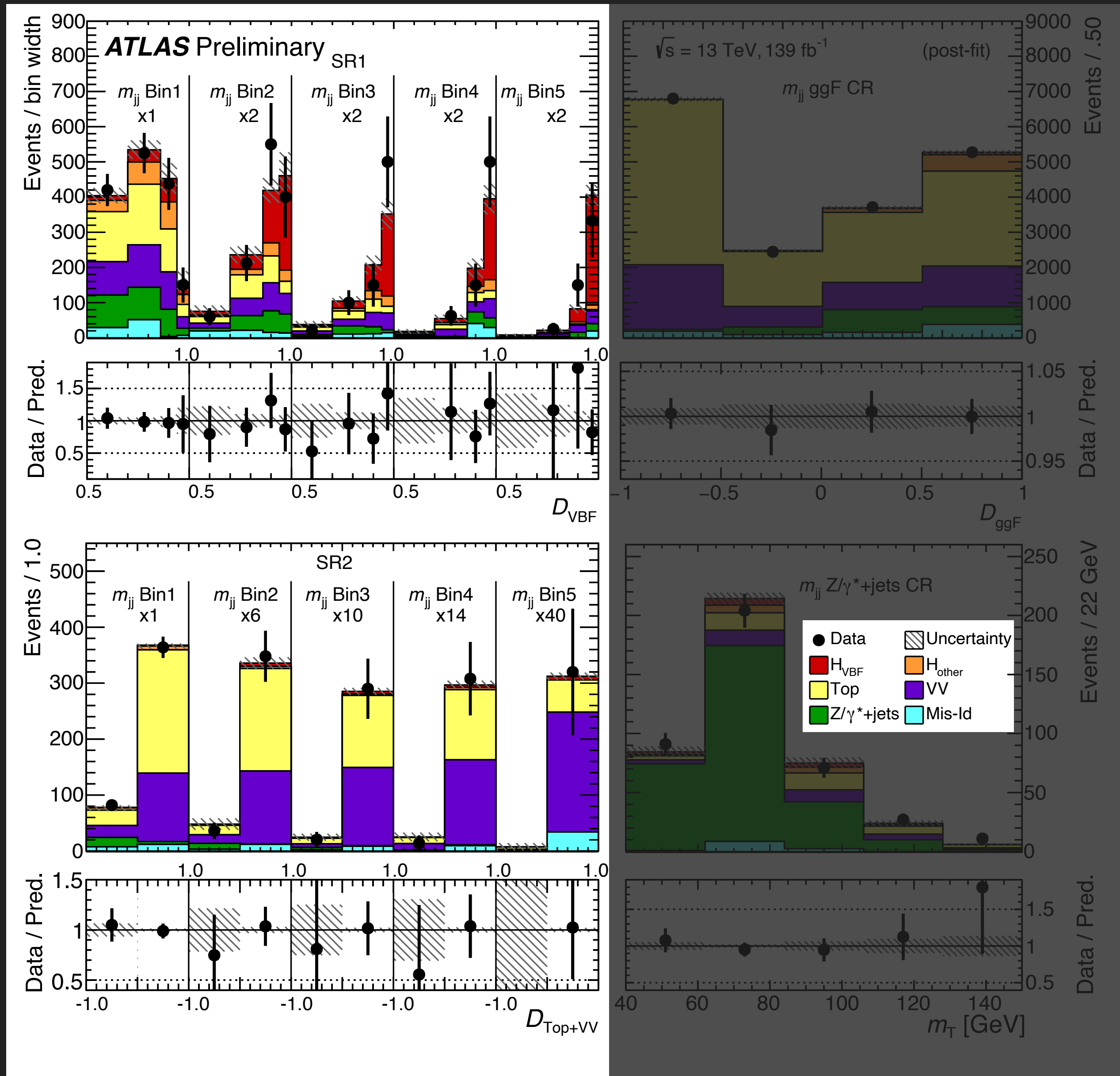
SR split in the fit template:

- SR1 rich in VBF signal.
- SR2 rich in top and VV.

D_{VBF} - VBF signal against Top+VV.



D_{top+VV} - Top+VV against all other processes.

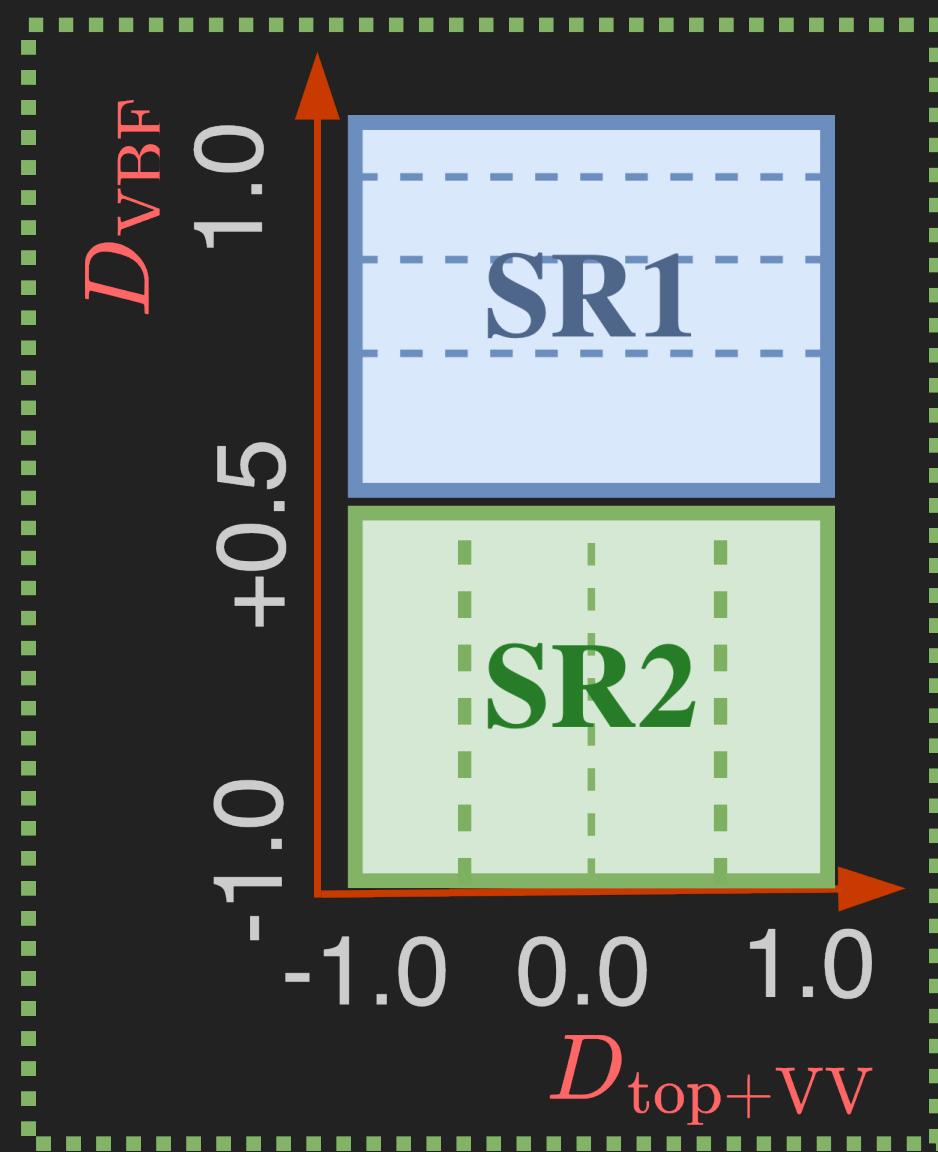


SIGNAL EXTRACTION STRATEGY

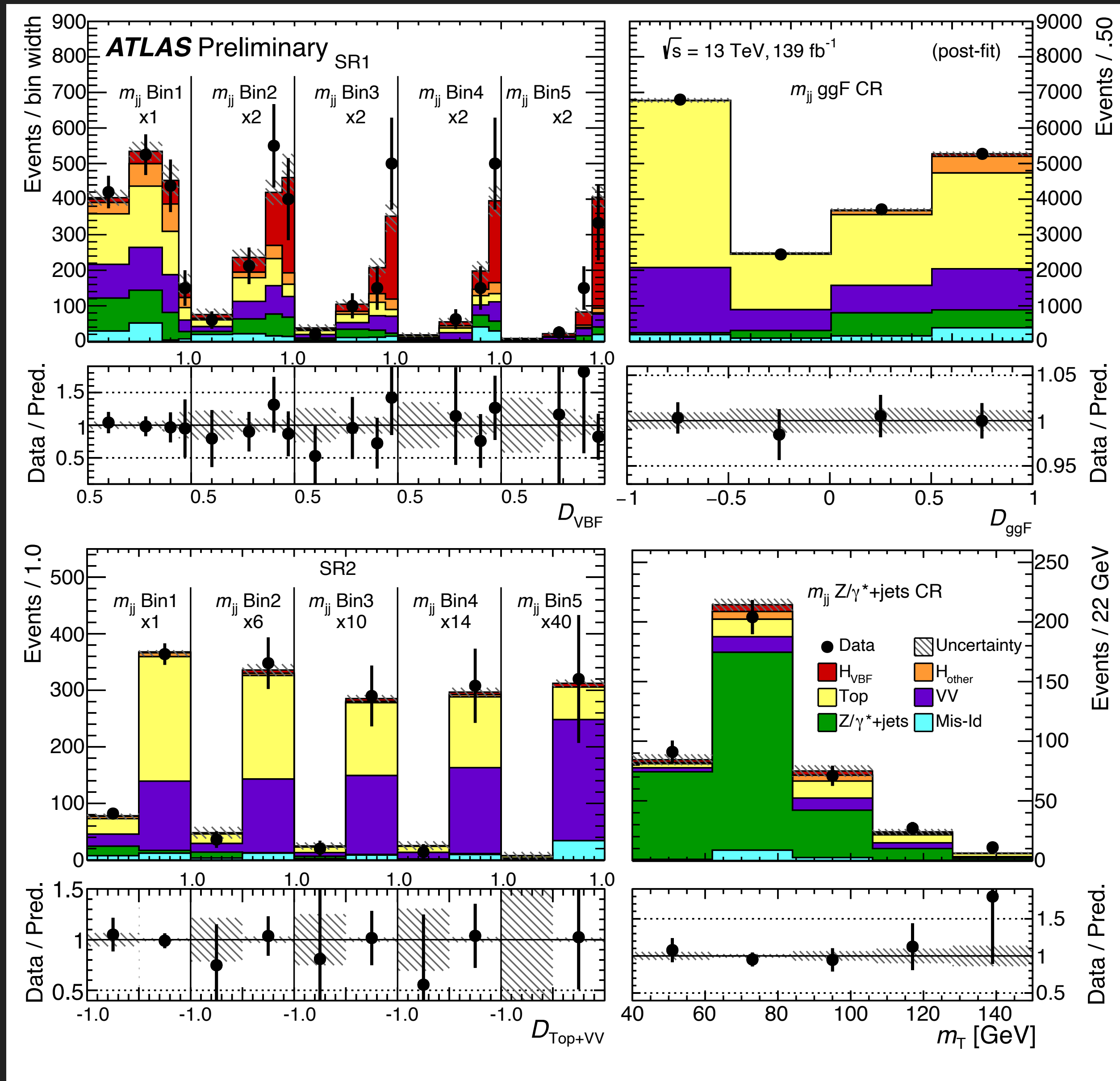
SR split in the fit template:

- SR1 rich in VBF signal.
- SR2 rich in top and VV.

D_{VBF} - VBF signal against Top+VV.

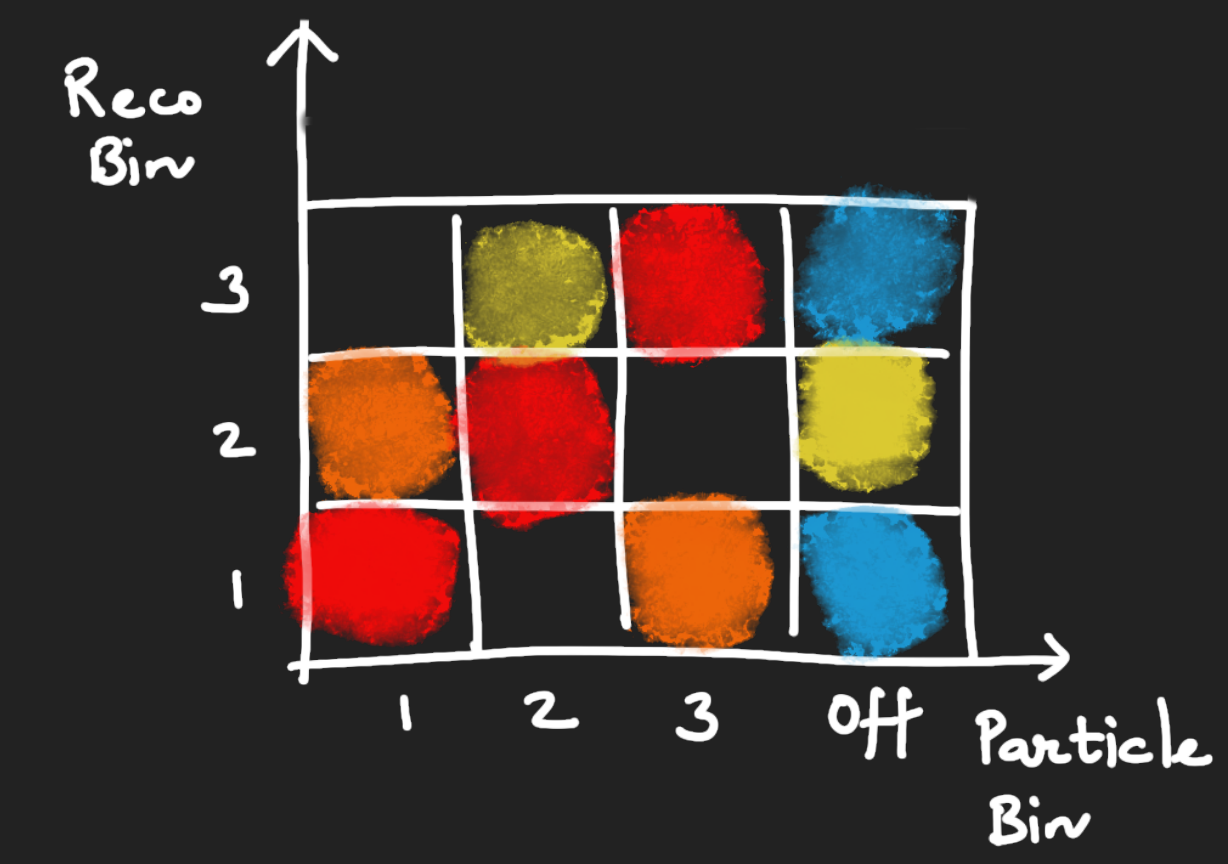


D_{top+VV} - Top+VV against all other processes.



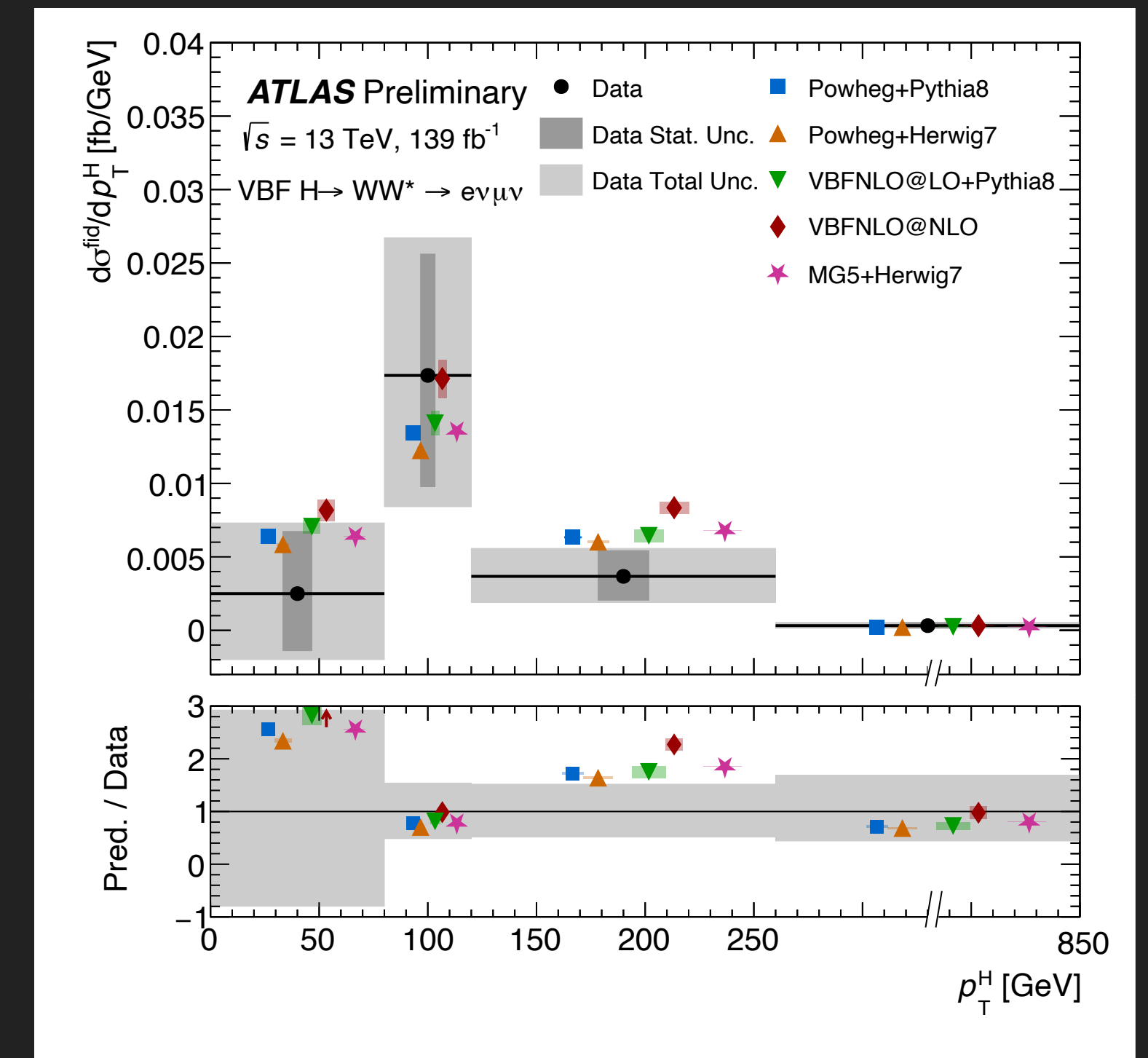
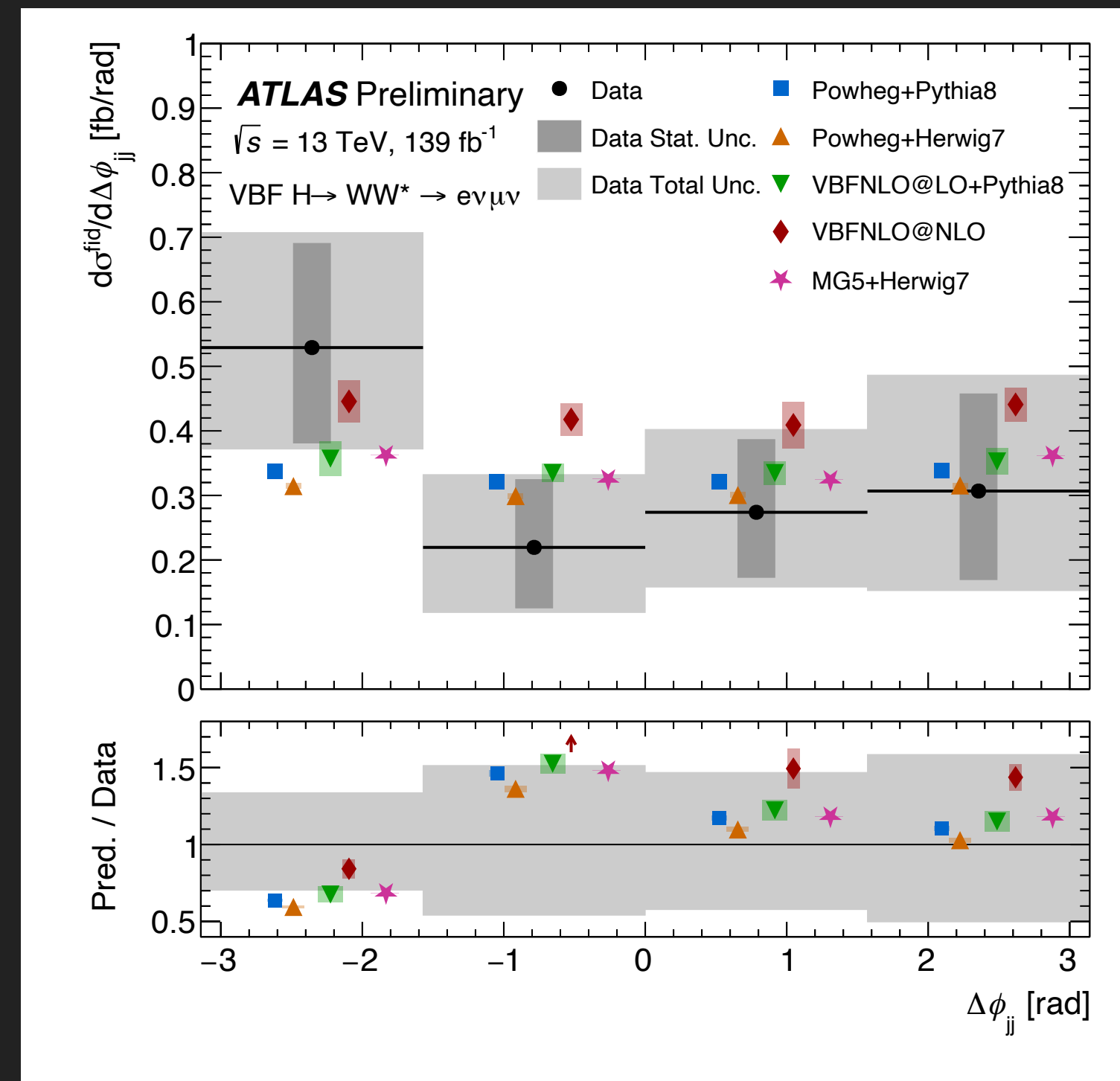
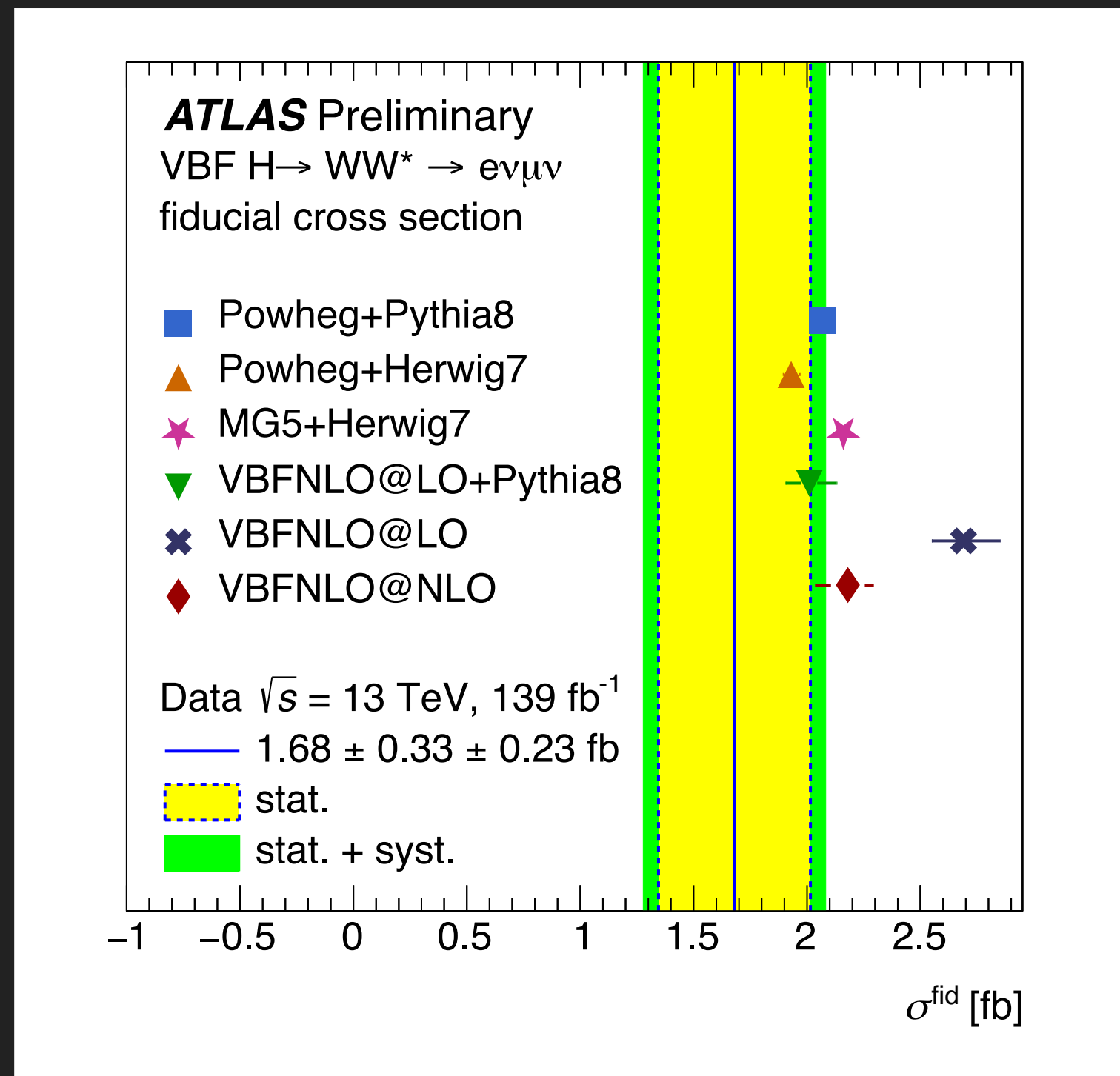
D_{ggF} - ggF background against all other processes.

Data driven estimates also for ggH and Z/γ^* +jets bkg.



Unregularized matrix-based unfolding in the same step as the likelihood fit

13 differential cross-sections measured – lepton kinematics, jet kinematics, and combined



Results compatible with SM predictions, limited by statistical uncertainty.

- Constraints are set on mass dim-6 Wilson coefficients (7 CP-even, 3 CP-odd) within the SMEFT formalism.

- One parameter constrained at a time.

$$\sigma - \sigma_{\text{SM}} \propto 2 \sum_i \frac{c_i}{\Lambda^2} \text{Re} \left(\mathcal{M}_{\text{SM}}^* \mathcal{M}_i \right) + \sum_{i,j} \frac{c_i c_j}{\Lambda^4} \text{Re} \left(\mathcal{M}_i^* \mathcal{M}_j \right)$$

1 TeV

Linear Term

Quadratic Term

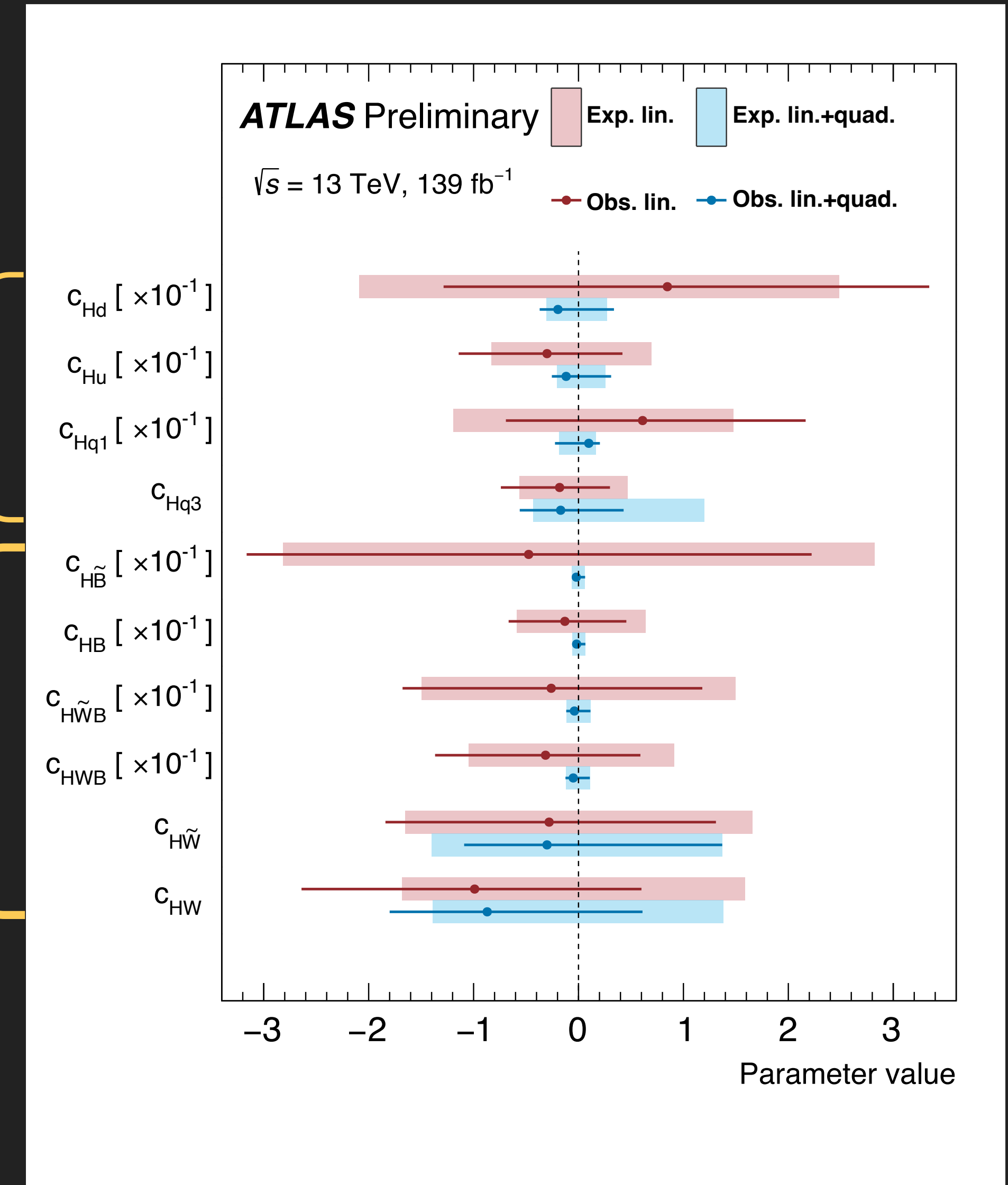
- Stronger limits from the linear+quadratic parameterization compared to linear only.

- Shows the impact of the quadratic term (and hence possible sensitivity to higher mass dimension terms).

Observable Used

$p_T^{j_1}$

$\Delta\phi_{jj}$

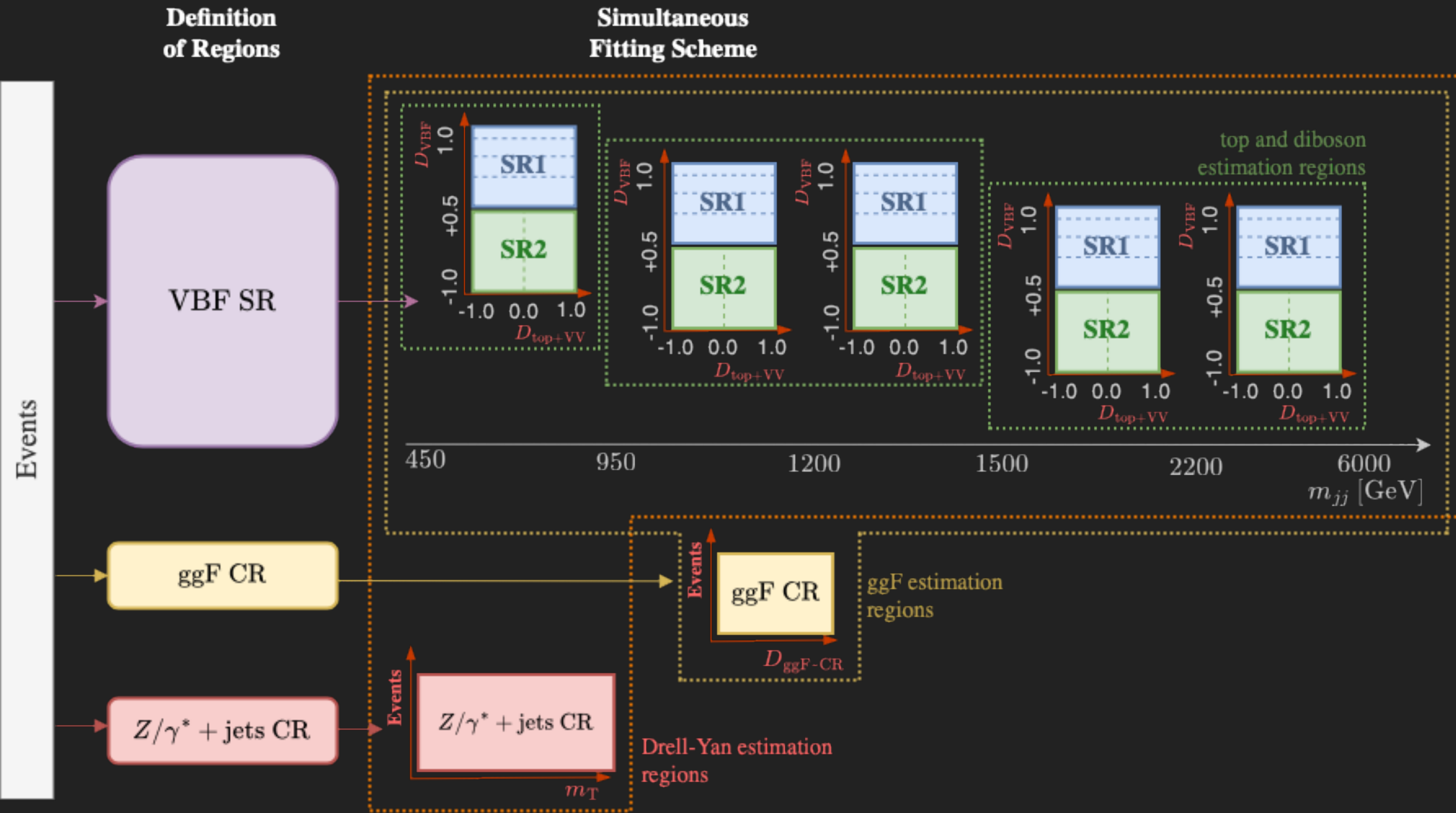


Thank you for listening!

[CERN-EP-2023-25](#)

ADDITIONAL MATERIAL

Selection Requirements	Signal Region	Fiducial Region
Lepton pair flavors	$e-\mu$	
Lepton pair charge	0	
Leading (subleading) lepton p_T	> 22 GeV (> 15 GeV)	
Lepton η^ℓ	$ \eta^\mu < 2.5$ $0 < \eta^e < 1.37$ or $1.52 < \eta^e < 2.47$	$ \eta^e < 2.5$
No. of additional leptons	0	
$\Delta R(\ell, \ell)$	overlap removal	> 0.1
$m_{\ell\ell}$	> 10 GeV	
$\Delta R(\ell, \text{jet})$	overlap removal	> 0.4
No. of jets ($p_T > 30$ GeV, $ \eta < 4.5$)	≥ 2	
No. of b -jets ($p_T > 20$ GeV, $ \eta < 2.5$)	0	
$m_{\tau\tau}$	$< m_Z - 25$ GeV	
Central jet veto ($p_T > 20$ GeV)	✓	
Outside lepton veto	✓	
m_{jj}	> 450 GeV	
$ \Delta y_{jj} $	> 2.1	
$ \Delta\phi_{\ell\ell} $	< 1.4 rad	



Background	Estimation
Diboson	Data-driven
Top Induced	Data-driven
ggF H	Data-driven
Z+Jets	Data-driven
W+Jets (Mis-Id)	Data-driven
$V\gamma$	MC
Htt, VH	MC

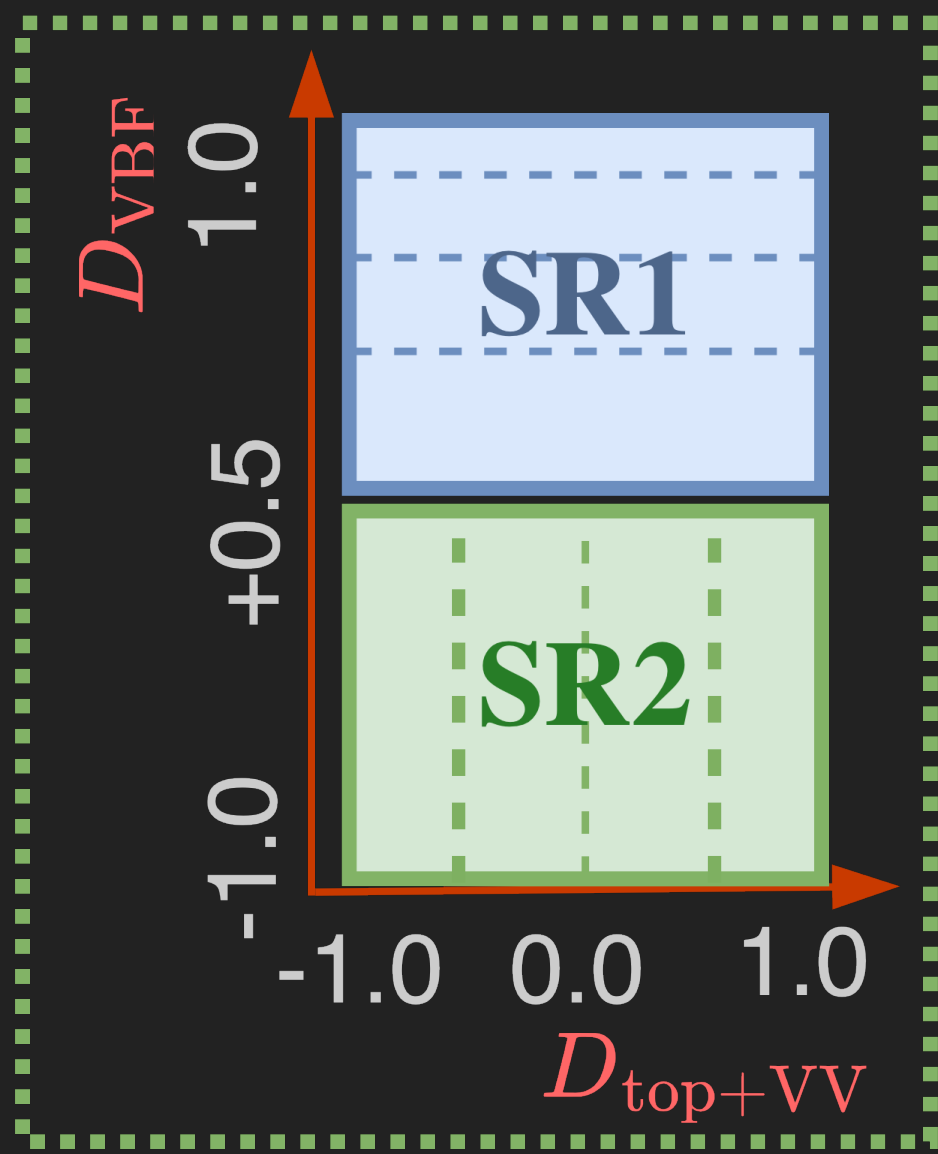
Scheme designed to **minimize total uncertainty**.
 Comes at a cost of slight increase in stat. unc., but significant reduction in syst. unc.

BACKUP

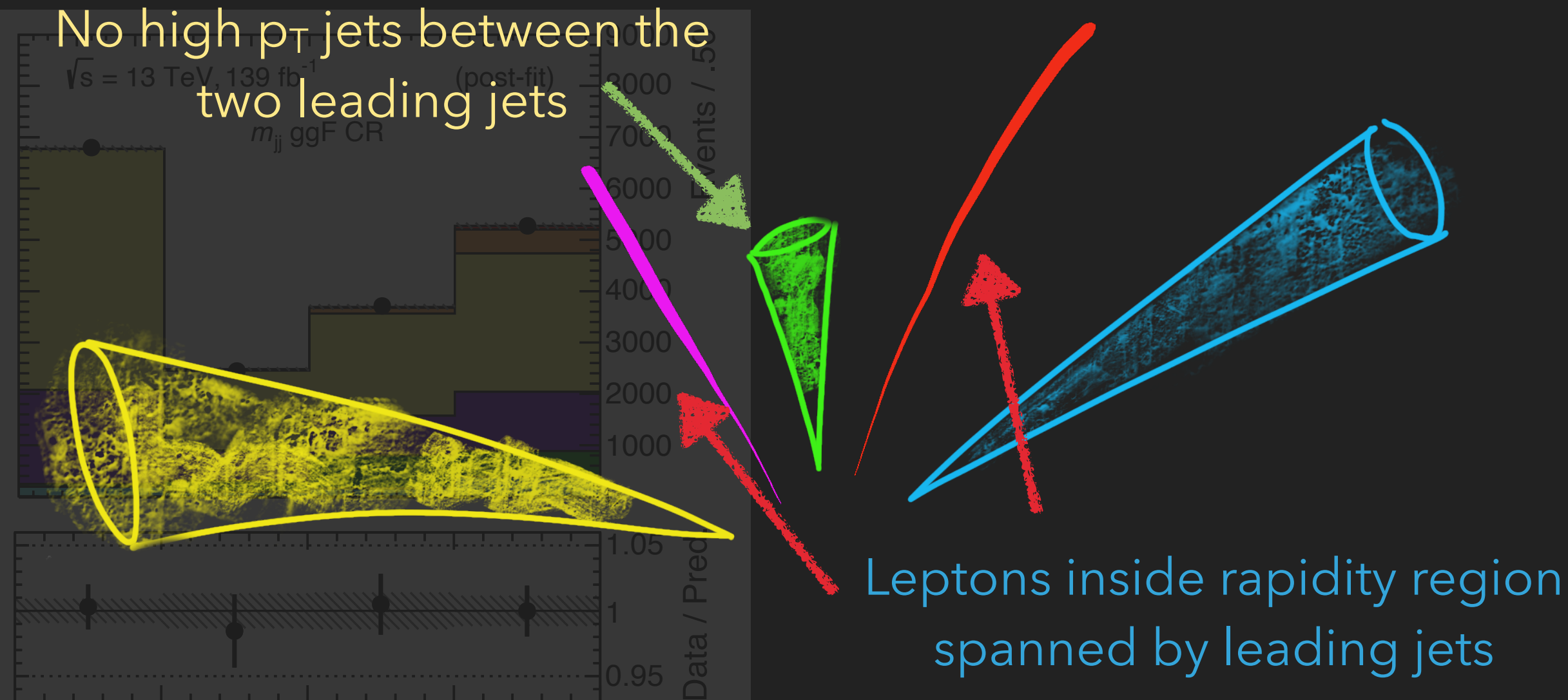
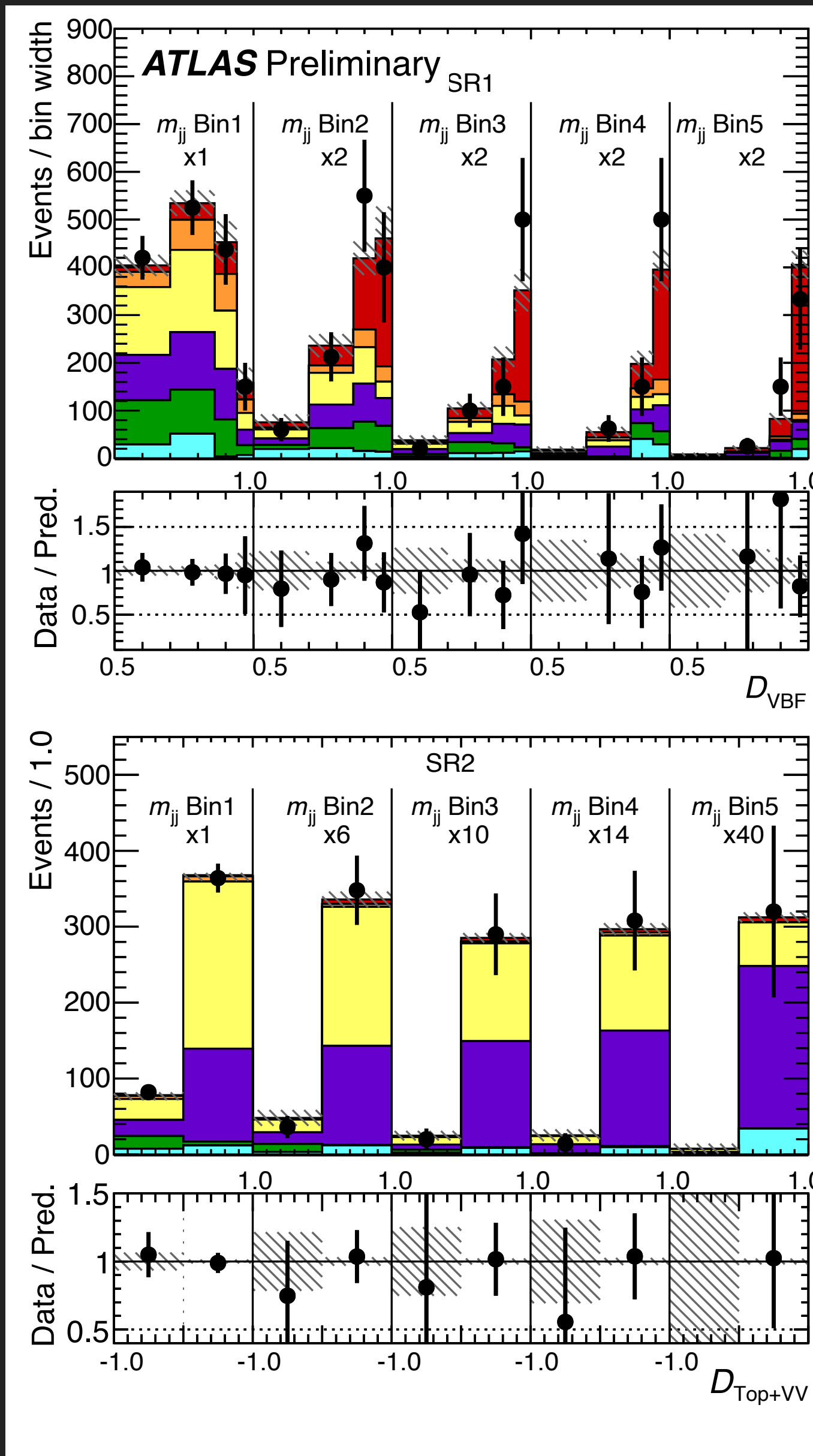
SR split in the fit template:

- SR1 rich in VBF signal.
- SR2 rich in top and VV.

D_{VBF} - VBF signal against Top+VV.



D_{top+VV} - Top+VV against all other processes.



Estimating bkg from the same phase space of the measurement significantly reduces extrapolation unc.

$m_{\tau\tau}$	$< m_Z - 25 \text{ GeV}$
Central jet veto ($p_T > 20 \text{ GeV}$)	yes
Outside lepton veto	yes
m_{jj}	$> 450 \text{ GeV}$
$ \Delta y_{jj} $	> 2.1
$ \Delta \phi_{ll} $	$< 1.4 \text{ rad}$

Reconstruction-level cuts in the SR

$m_{\tau\tau}$
 Central jet veto ($p_T > 20\text{GeV}$)
 Outside lepton veto
 $|\Delta\phi_{\ell\ell}|$

$< m_Z - 25\text{ GeV}$
 Exactly 1 fails
 $< 1.4\text{ rad}$

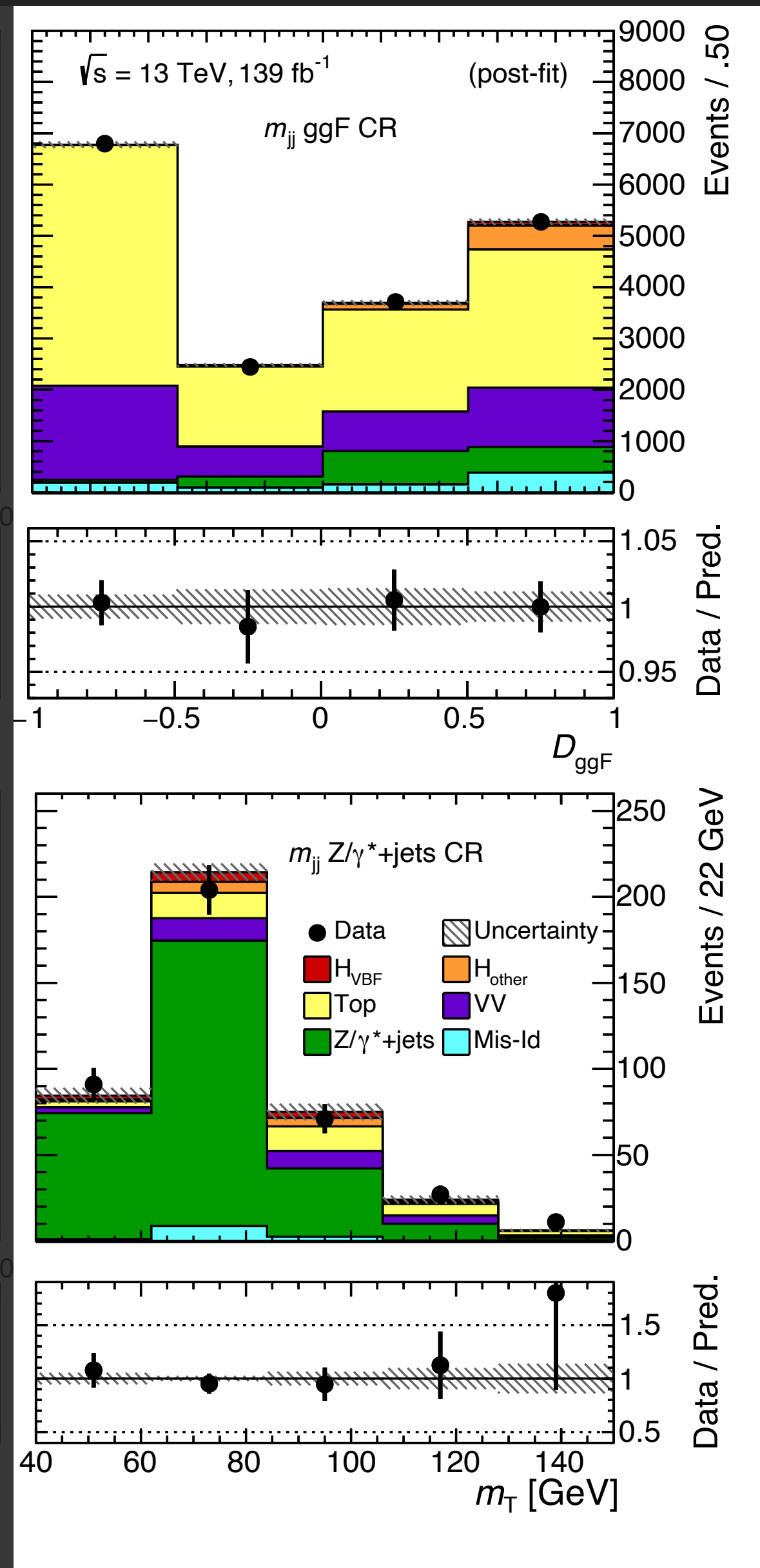
ggF CR definition

Sample	SR	Z/ γ^* +jets CR	ggF CR
Signal (POWHEG+PYTHIA 8)	110	13	86
ggF Higgs	39	4	450
Other Higgs	3	10	78
Top	420	41	11 000
Z/ γ^* +jets	79	320	1 400
VV	280	32	4 300
V γ	13	14	210
Mis-Id	47	12	810
Total Signal+Background	1 000 \pm 120	450 \pm 160	18 800 \pm 2 600
Data	916	406	18 228

$m_{\tau\tau}$
 Central jet veto ($p_T > 20\text{GeV}$)
 Outside lepton veto
 m_{jj}
 $m_{\ell\ell}$

$66.2\text{ GeV} < m_{\tau\tau} < 116.2\text{ GeV}$
 yes
 yes
 $> 450\text{ GeV}$
 $< 80\text{ GeV}$

Z/ γ^* +jets CR definition



D_{ggF} - ggF background against all other processes.

μ_{ggF} estimated in ggF CR and SR

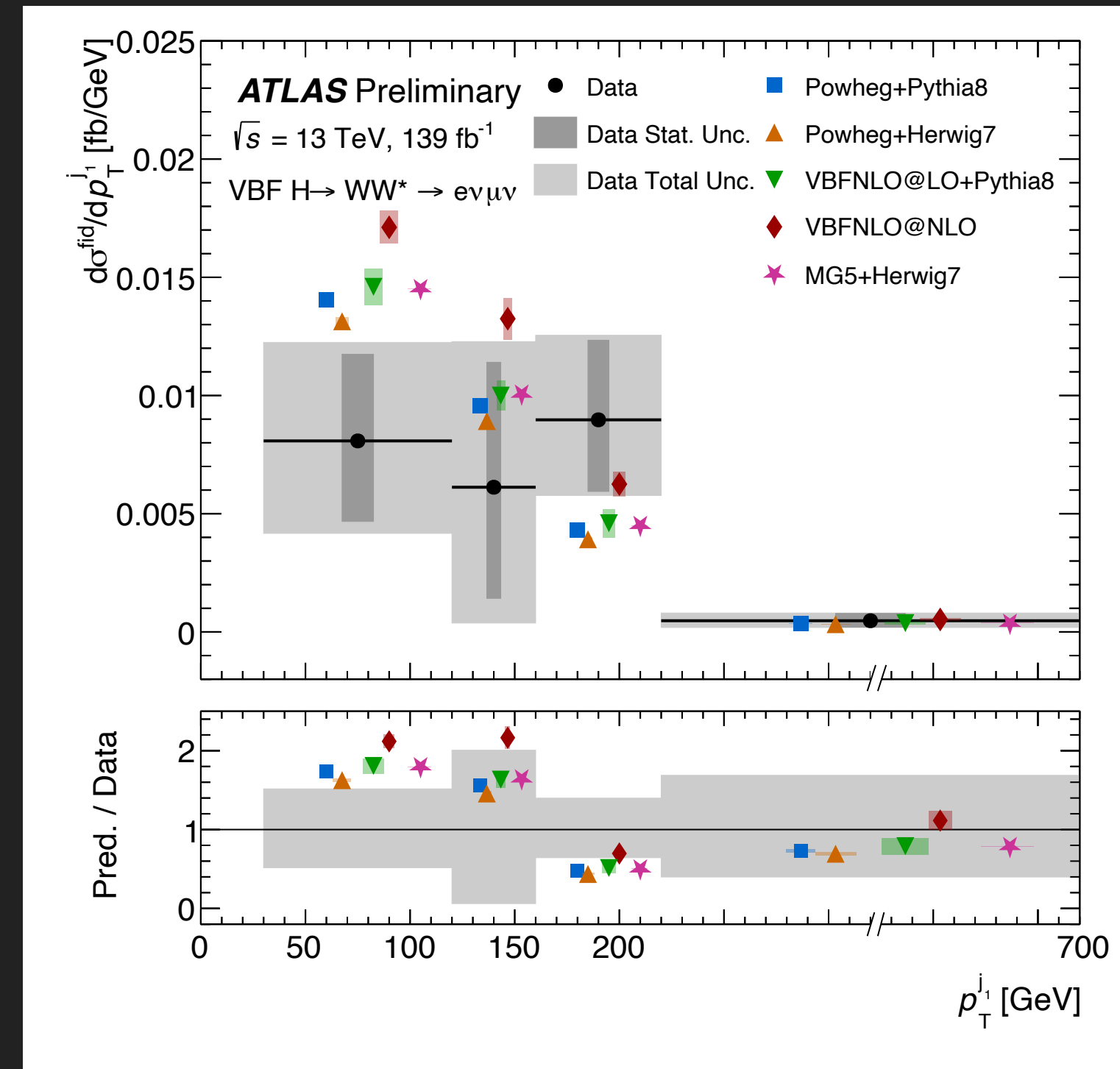
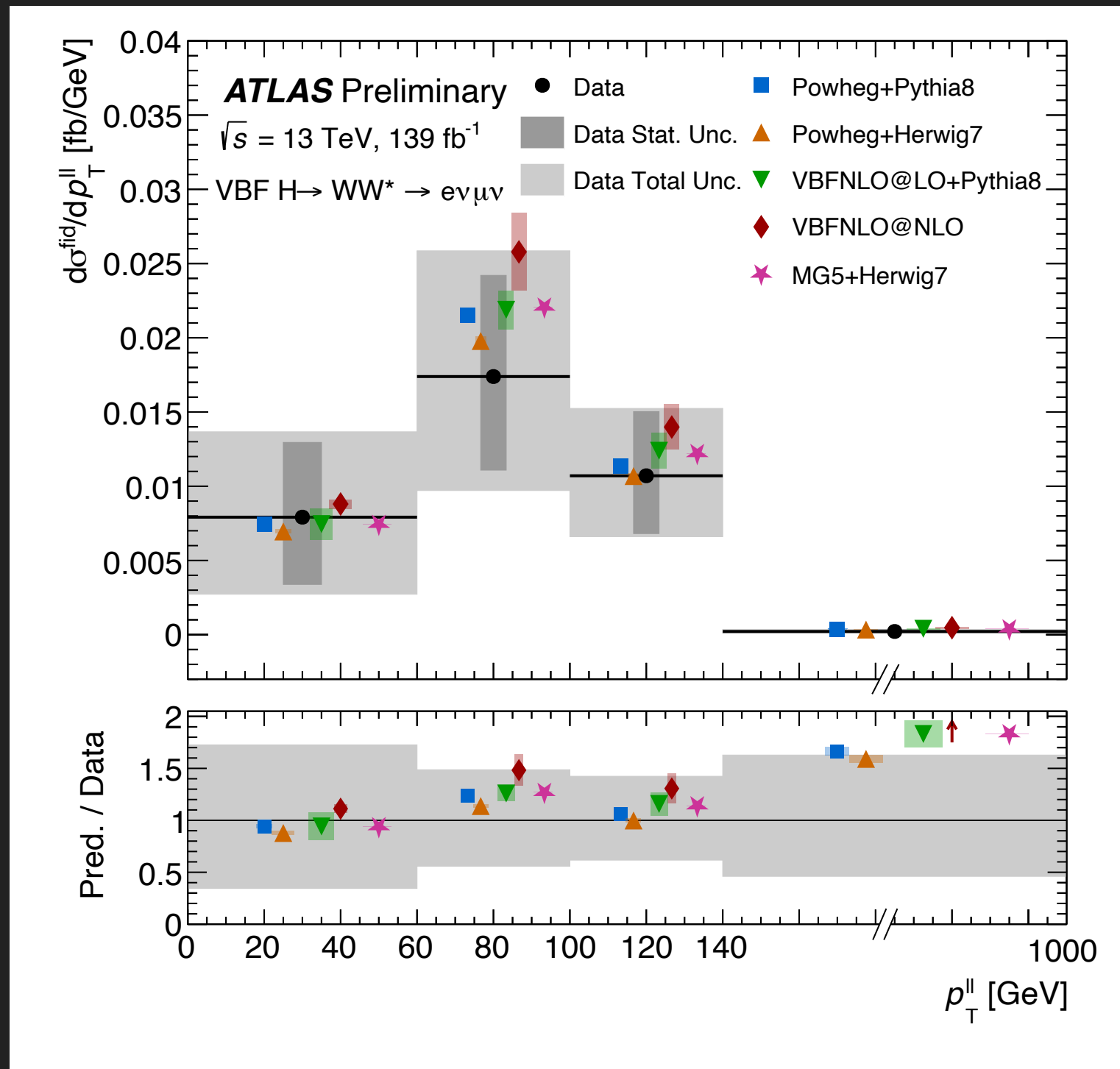
W+jets CR used to estimate the contribution from jets mis-reconstructed as leptons.

$\mu_{\text{Z+jets}}$ estimated in Z/ γ^* +jets CR and SR

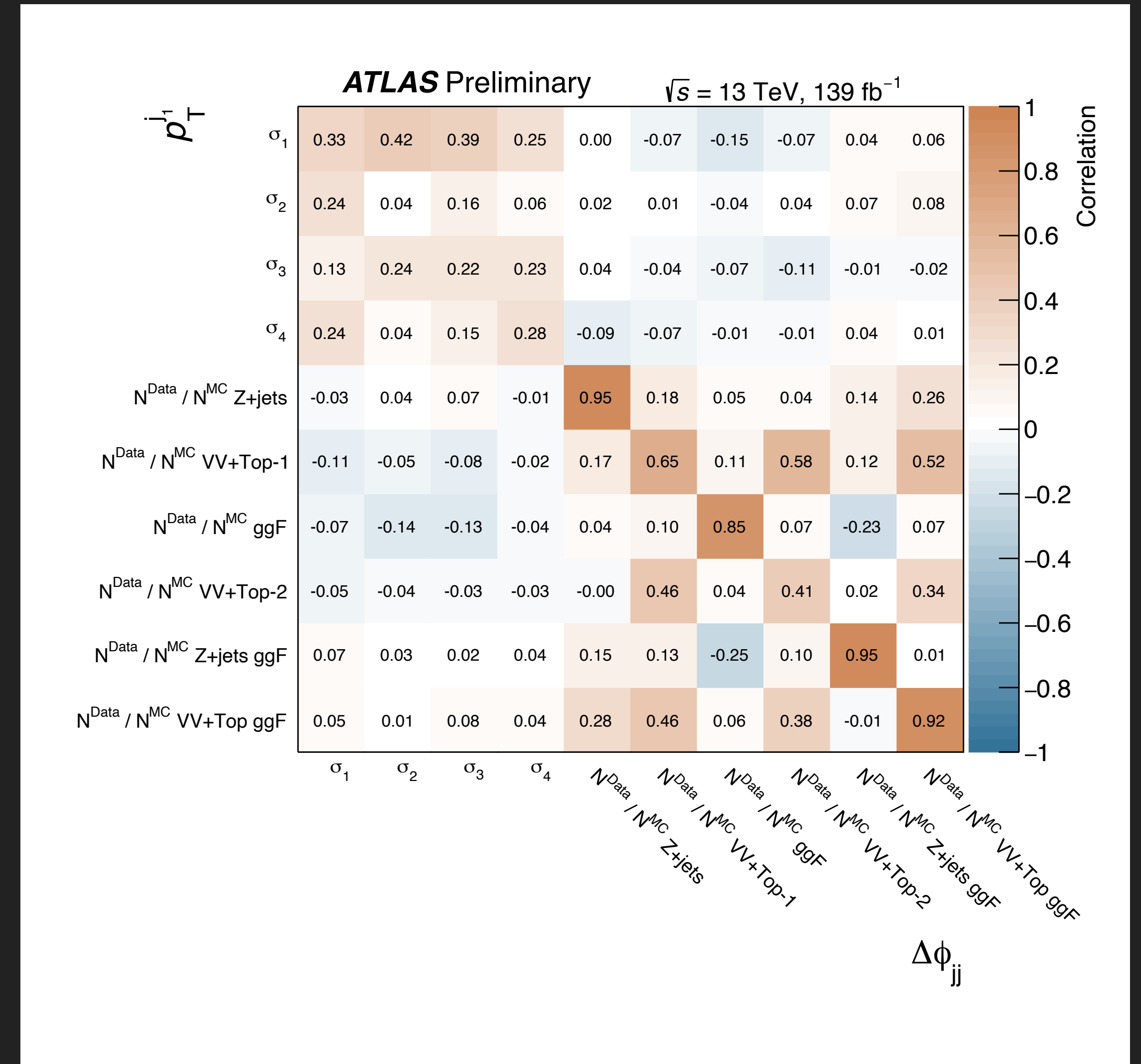
- Measurements **limited by data statistics**.
- Inclusive XS measurement limited by (in order) -
 - Data statistics,
 - Background modeling ($t\bar{t}$ PS/UE and matching),
 - Signal modeling (**generator**),
 - Jets (**JER**), pileup, and MET,
 - MC stats.

Source	Uncertainty [%] σ^{fid}	Uncertainty range [%]				
		p_T^H	$p_T^{\ell\ell}, p_T^{\ell_1}, p_T^{\ell_2}, \Delta y_{\ell\ell} , \Delta\phi_{\ell\ell} , \cos(\theta_\eta^*)$	$m_{\ell\ell}$	$p_T^{j_1}, p_T^{j_2}, \Delta y_{jj} , \Delta\phi_{jj}$	m_{jj}
Signal modelling	5	< 1 – 7	< 1 – 7	< 1 – 19	< 1 – 8	2 – 7
Signal parton shower	< 1	< 1 – 2	< 1 – 1.8	< 1 – 10	< 1 – 1.8	< 1 – 7
$t\bar{t}$ modelling	6	1.7 – 30	3 – 13	3 – 80	3 – 10	1.2 – 70
WW modelling	4	< 1 – 12	3 – 11	2 – 90	3 – 10	3 – 40
Z/ γ^* +jets modelling	4	< 1 – 19	2 – 18	4 – 30	3 – 13	2 – 50
ggF modelling	5	4.0 – 28	3.4 – 10	2.6 – 12	2.3 – 9.0	1.4 – 86
Mis-Id. background	< 1	< 1 – 12	1.1 – 5	< 1 – 19	1 – 3	< 1 – 40
Jets & Pile-up & E_T^{miss}	5	8 – 60	6 – 30	6 – 120	9 – 30	9 – 130
b -tagging	< 1	< 1 – 9	< 1 – 3	< 1 – 19	1.1 – 3	< 1 – 40
Leptons	1.5	3 – 17	2 – 9	1.2 – 13	1.7 – 7	< 1 – 16
Luminosity	1.5	1.7 – 2	1.3 – 1.9	< 1 – 4	1.5 – 2	< 1 – 1.9
MC statistics	5	10 – 40	6 – 30	6 – 180	8 – 30	7 – 90
Total systematics	13	19 – 90	13 – 60	12 – 180	15 – 50	15 – 200
Data statistics	20	50 – 160	30 – 110	30 – 400	40 – 100	50 – 300
Total uncertainty	23	50 – 190	40 – 120	30 – 500	40 – 100	50 – 400

Post-fit uncertainty range for all the measurements



- Correlations between differential XS and background normalizations for all observables measured evaluated using the bootstrapping technique.
- Same procedure also used to evaluate correlations between central values of EFT operators.
- Correlations extremely useful for future global fits and EFT interpretations using more than one observable.
- All correlations as well as all individual correlated measurements published on HepData.



Wilson Coeff.	Operator Structure	Fit distr.
c_{HW}	$H^\dagger H W_{\mu\nu}^n W^{n\mu\nu}$	$\Delta\phi_{jj}$
c_{HB}	$H^\dagger H B_{\mu\nu} B^{\mu\nu}$	$\Delta\phi_{jj}$
c_{HWB}	$H^\dagger \tau^n H W_{\mu\nu}^n B^{\mu\nu}$	$\Delta\phi_{jj}$
c_{Hq1}	$(H^\dagger i \overleftrightarrow{D}_\mu H)(\bar{q}\gamma^\mu q)$	p_T^{j1}
c_{Hq3}	$(H^\dagger i \overleftrightarrow{D}_\mu^n H)(\bar{q}\tau^n \gamma^\mu q)$	p_T^{j1}
c_{Hu}	$(H^\dagger i \overleftrightarrow{D}_\mu H)(\bar{u}\gamma^\mu u)$	p_T^{j1}
c_{Hd}	$(H^\dagger i \overleftrightarrow{D}_\mu H)(\bar{d}\gamma^\mu d)$	p_T^{j1}
$c_{H\tilde{W}}$	$H^\dagger H \tilde{W}_{\mu\nu}^n W^{n\mu\nu}$	$\Delta\phi_{jj}$
$c_{H\tilde{B}}$	$H^\dagger H \tilde{B}_{\mu\nu} B^{\mu\nu}$	$\Delta\phi_{jj}$
$c_{H\tilde{W}B}$	$H^\dagger \tau^n H \tilde{W}_{\mu\nu}^n B^{\mu\nu}$	$\Delta\phi_{jj}$

Operator structure corresponding to the constrained Wilson coefficients